Available online at www.sciencedirect.com
SCIENCE DIRECT®
Journal of Chromatography A, 1037 (2004) 405–410
JOURNAL OF CHROMATOGRAPHY A
www.elsevier.com/locate/chroma

Review

Physicochemical properties of enhanced-fluidity liquid solvents

Susan V. Olesik*

Department of Chemistry, The Ohio State University, 100 West 18th Avenue, Columbus, OH 43210, USA

Abstract

Enhanced fluidity (EF) liquid mixtures are advantageous as mobile phases for the separation of moderate to polar compounds in liquid chromatography (reversed-phase, normal, size exclusion, size exclusion, and chiral separations). The low viscosities and high diffusivities of EF mixtures allow highly efficient separations to be achieved in a small amount of time. The best use of enhanced-fluidity liquids is only possible when their physicochemical properties are known. Herein, the techniques used to measure the physicochemical properties (phase diagram, diffusivity, solvent strength and pH) of EF liquids are described. For each technique, the experiment design and the care necessary to insure the quality of the collected data are described. Finally, the impact of the measured physicochemical properties on the chromatography is also highlighted.

Keywords: Reviews; Enhance-fluidity liquid solvents; Mobile phase composition

Contents

1. Introduction

Enhanced-fluidity liquid mixtures are polar liquids to which high proportions of soluble gases have been added. The gases are completely dissolved in the liquid. These mixtures share many of the positive attributes of both liquids and supercritical fluids. For example, a mixture of methanol–CO_2 (50:50, w/w) has approximately the same polarity as methanol with a viscosity that is 70% of the viscosity of methanol. Similar to the properties of supercritical fluids, the polarity of enhanced-fluidity liquids can be varied by changing the applied pressure. In addition, enhanced-fluidity liquid mixtures require low applied pressures to maintain a single-phase mixture.

Enhanced-fluidity liquid chromatography (EFLC) has been used in reversed-phase and normal-phase HPLC as well as for size exclusion separations [1]. Improved chromatographic efficiency and speed of analysis were observed in these studies. Substantial improvements were also observed when EFLC was used for chiral separations [2]. EFLC was found to be markedly more efficient and often have higher selectivity than when using supercritical fluid chromatography or conventional HPLC. The low viscosity of EF liquids has also allowed the use of long (1 m or more) capillary columns to produce highly efficient separations [3].

Knowledge of the physicochemical properties of enhanced-fluidity liquids is essential to correctly choosing operating conditions for a given separation. A combination of chromatographic and spectrophotometric methods has been used to garner this information. Herein, the properties of enhanced-fluidity liquids are described along with a

* Corresponding author. Tel.: +1-614-2920733; fax: +1-614-2921685.
E-mail address: olesik.1@osu.edu (S.V. Olesik).

0021-9673/$ – see front matter © 2004 Elsevier B.V. All rights reserved.
doi:10.1016/j.chroma.2004.04.001

description of the methods used to determine those properties, and the possible applications of the different types of EF mixtures are described.

2. Phase diagrams

The most common means of determining phase diagrams is to use a variable volume, optical view cell and look for the occurrence of phase boundaries. By varying either temperature, pressure or both for a mixture of known composition, the phase boundaries are readily determined. A stainless steel variable volume, variable temperature, optical view cell was used previously to determine the phase diagrams of methanol–CO_2, acetonitrile–CO_2 [4], methanol–water–CO_2, acetonitrile–water–CO_2 [5], tetrahydrofuran–CO_2 [6], methanol–fluoroform, and methanol–water–
fluoroform [7].

The 0–35 mL stainless steel optical cell is rated to allow a maximum temperature of 177 °C and a maximum pressure of 585 atm (atm $\times$ 1.0135 $\times$ 10^5 = Pa) (purchased from Temco, Inc., Tulsa, OK, USA). With the temperature controller (CN 9000 series from Omega, Engineering, Stamford, CT, USA) used the cell temperature is controlled to ±0.1 °C and the pressure of the fluid is monitored from 1 to 340 atm with an accuracy of ±0.4 atm) with a Setra 204 pressure transducer (Setra Systems, Inc., Acton, MA, USA) which was calibrated in the factory relative to NIST standards (National Institute of Standards and Technology, Gaithersburg, MD, USA) [1].

This is a method of phase boundary determination that allows phase transitions to be readily observed. With this type of instrumentation, care must be taken to use O-ring seals that do not leach into the pure solvent. Also, the temperature of the fluid must be measured directly in the fluid and not on the outside portion of the vessel.

Possible enhancements to this type of instrumentation include the use of laser scattering to detect the onset of phase demixing [8]. However, if very accurate phase boundaries are desired, the laser light scattering method may not be the best choice because it may incorrectly identify the boundary. The presence of very small droplets of one phase adhering to an O-ring or at or in the crevice of the cell may be the first sign of the demixing of the components in the cell. This is not readily detected by a laser beam that is typically positioned at the center of an optical flow cell.

Fig. 1A shows the methanol–CO_2 phase diagram at 25, 50, and 80 °C [1]. The single phase region is above the data points. Fig. 1B shows the methanol–fluoroform phase diagram for the same three temperatures [4]. Note the shape of the two phase diagrams is similar. However, for a given mixture composition, the methanol–fluoroform mixtures require less applied pressure to stay in the one phase region than the methanol-CO_2 mixtures. Fig. 1C is the phase diagram for the tetrahydrofuran–CO_2 mixture for the same temperatures. The shapes of the isotherms are different from the other two in that only at the 80 °C does the coexistence curve level off like what is observed for the methanol–fluoroform and methanol–CO_2 mixtures. However, the most important attribute of these phase diagrams for separation science applications is the fact that the pressure necessary to maintain single phase conditions is relatively low, <150 atm, for all three mixtures over the illustrated temperature range.

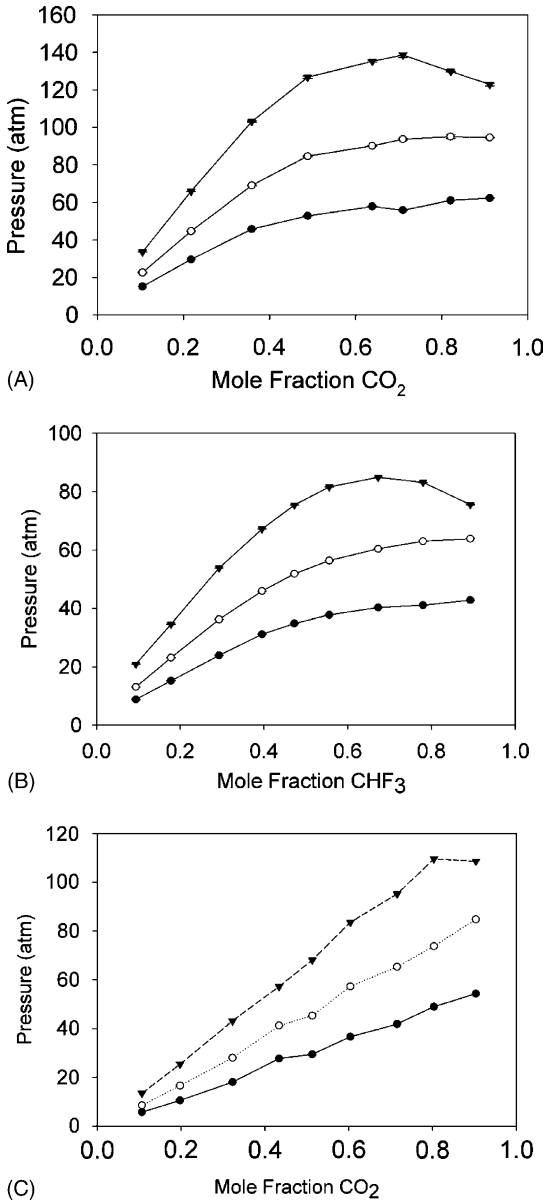

Fig. 1. Vapor–liquid equilibrium isotherms: (A) methanol–CO_2 at 25, 50 and 80 °C; (B) methanol–CHF_3 at 25, 50 and 80 °C; (C) tetrahydrofuran–CO_2 at 25, 50 and 80 °C.

Fig. 2A shows the methanol–water–CO_2 phase diagram at 25 °C [2]. These mixtures are single phase left and above the curve shown. The *R*-value is the ratio of moles of water to mole of methanol. As the *R*-value increases the moles fraction of carbon dioxide that is miscible decreases. Fig. 2B shows the phase diagram of methanol–water–fluoroform at

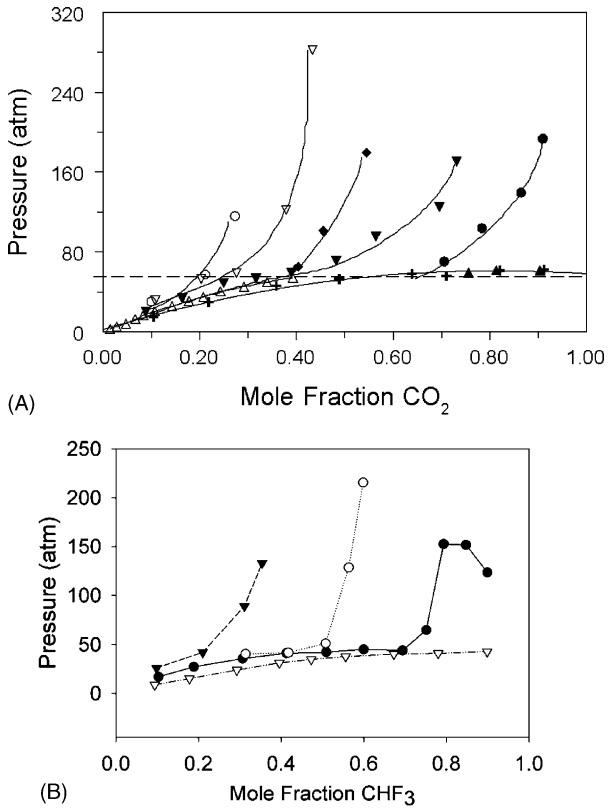

Fig. 2. Vapor–liquid equilibrium isotherms: (A) methanol–water–CO_2 at 25 °C for (+) $R = 0.000$, (△) $R = 0.1197$, (●) $R = 0.1810$, (▼) $R = 0.2490$, (◇) $R = 0.3318$, (▽) $R = 0.4298$, (○) $R = 0.5633$; (B) methanol–water–CHF_3 at 25 °C for (+) $R = 0.000$, (●) $R = 0.2571$, (■) $R = 0.3960$, (▼) $R = 0.5710$, where R = moles water/moles methanol.

25 °C [4]. The isotherms for this mixture are remarkable similar to those for methanol–water–CO_2, especially considering the large difference in polarity between fluoroform and carbon dioxide. The complete analysis of the phase behavior for methanol–water–CO_2 showed that higher proportions of fluoroform were soluble in methanol–H_2O mixtures than observed for CO_2 [4].

3. Diffusion coefficients

The rate of mass transfer of analytes at near infinite dilution conditions in enhanced-fluidity liquid mixtures was determined using the chromatographic band broadening procedure developed by Giddings and Seager [9]. In this procedure, a solution of the analyte dissolved in the mobile phase solvent is injected into a capillary tube and is eluted as a Gaussian peak. The band of the peak is related to the diffusion coefficient through the following equation:

$$\sigma_L^2 = \frac{2D_{12}L}{u} + \frac{d_c^2 uL}{96D_{12}} \quad (1)$$

where σ_L^2 is the spatial variance (units of cm^2) of the Gaussian peak, L is the length of the capillary, D_{12} is the binary diffusion coefficient of the solute at infinite dilution conditions, u is the average linear velocity of the mobile phase, d_c is the diameter of the column. Because the magnitude of the diffusion coefficients in enhanced-fluidity liquids is small (typically $10^{-4}\,cm^2/s$), the first term in the above equation is negligible and the linear velocity, u, is L/t_r, where t_r is the center of mass of the chromatographic band in units of time. In addition, since the retention factor is zero in an open tube, L^2/σ_L^2 can be replaced with t_r^2/σ_t^2, where σ_t^2 is the temporal variance (units of s^2). Therefore, the resulting equation used to determine the diffusion coefficients in enhanced-fluidity liquids is:

$$D_{12} = \frac{d_c^2 L^2}{96 t_r \sigma_L^2} \quad (2)$$

where all of the terms are determined experimentally. Values of t_r and σ_t^2 are determined from the first and second statistical moment of the eluted peak. Peak injection and measurement is then repeated 10–15 times which results is relative standard deviation of the diffusion coefficient of ±5%. This treatment assumes that secondary flow is not contributing to the band dispersion and that is ensured by making certain that the aspect ratio (ratio of coil diameter/coil internal diameter) is high. The solvent used to inject the analyte into the tube must be the same solvent as the running mobile phase and the analyte concentration in the injected solvent should as low as possible (using conditions near a $S/N = 2$ for the detector) to insure that the measured diffusion coefficients represent correct binary diffusion coefficients (diffusion coefficients of the analyte in the mobile phase). Finally, to insure accuracy of the measured diffusion coefficients, the diffusion coefficients with known values should be measured with the configured instrument to verify the accuracy of the measurement. We chose to confirm the quality of the method by measuring the diffusion coefficient of benzene in supercritical CO_2 at 40 °C because that value has been measured and verified by others [10–12].

Fig. 3 shows the variation of the diffusion coefficient of benzene in methanol–water–CO_2 mixtures of methanol–water (0.70:0.30 mole fraction) and methanol–water–CO_2 (0.49:0.21:0.20 to 0.42:0.18:0.40 mole fraction) at 136 atm as a function of increasing temperature. The mole ratio of methanol–water was held constant at 2.3 for all of these mixtures while varying the mole fraction of CO_2 from 0 to 0.40. Note the substantial increase in the diffusion coefficient with increasing proportions of CO_2 and with increasing temperature. Interestingly, the largest diffusion coefficients were found near the phase boundaries for each mixture and the substantial increase of the diffusion coefficients for the enhanced-fluidity liquid mixtures was much greater than that predicted by Eyring rate theory [13]. When holding the mobile phase linear velocity constant, increasing the proportion of CO_2 from 0 to 0.30 mole fraction in the methanol–water–CO_2 mobile phase decreased the analysis time by half.

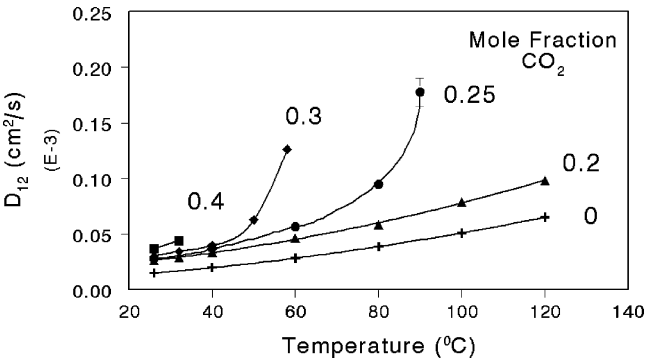

Fig. 3. Variation in diffusion coefficients of benzene in (+) 0.70/0.30 mole fraction methanol/water, (▲) 0.56/0.24/0.20 methanol/water/CO_2, (●) 0.52/0.23/0.25 methanol/water/CO_2, (◆) 0.49/0.21/0.30 methanol/water/CO_2 and (■) 0.42/0.18/0.40 methanol/water/CO_2.

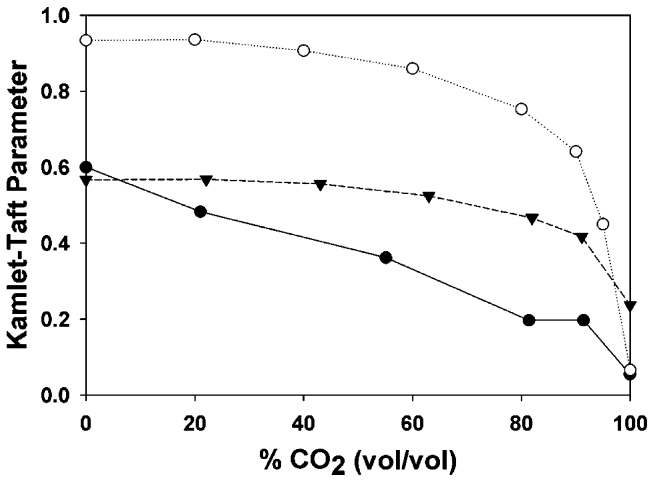

Fig. 4. Variation of Kamlet–Taft: (○) α, (▼) β, (●) π^*, parameters as a function of mixture composition for methanol–CO_2 mixtures at 25 °C and 170 atm.

4. Polarity of enhanced-fluidity liquid mixtures

4.1. Solvent polarity measured with solvatochromic parameters

The solvent strengths of the enhanced-fluidity liquid mixtures were determined by measuring the Kamlet–Taft (K–T) π^*, α, and β solvatochromic parameters. π^* is measure of the dipolarity and polarizability of the solvent; α is a measure of the hydrogen bond acidity, and β is a measure of hydrogen bond basicity. These parameters are measured by monitoring the shift in the UV-Vis spectrum of solvatochromic dye molecules. The values of the Kamlet–Taft, parameters are intended to vary with values of 0 to 1 with increasing polarity [14]. Therefore, a comparison of the Kamlet–Taft parameters for a given solvent describes the relative magnitudes of the intermolecular interactions. In comparison to other possible solvatochromic parameters, the Kamlet–Taft parameters have the advantage that they separate the specific intermolecular interactions.

Fig. 4 shows the variation of the Kamlet–Taft α, β and π^* parameter for the mixtures of methanol and CO_2 at 25 °C and 170 atm. The hydrogen bond acidity, α, and basicity, β, of the methanol–CO_2 mixtures are approximately that of the methanol even when up to 60–70 vol.% CO_2 is present in the mixture. The dipolarity– polarizability factor, π^* decreases more rapidly and approximately linearly with addition of up to approximately 80 vol.% CO_2 was added.

Fig. 5 shows the variation of the Kamlet–Taft π^* parameter for mixtures of methanol–water–CO_2. The most important attribute of the polarity studies of these mixtures is that the overall solvent strength remains high, as measured with the Kamlet–Taft α, β, and π^* parameters. However interestingly, while α and π^* decrease with increasing proportions of carbon dioxide, β increases.

These mixtures of methanol–water–CO_2 have been used to achieve high efficiency separations under reversed-phase LC conditions. In addition, as shown in the next section buffers of a broad range of pH can be produced in these mixtures which also provides significant flexibility for enhanced-fluidity, reversed–phase HPLC applications.

Mixtures of tetrahydrofuran and CO_2 were found to be useful mixtures for improving the efficiency in size exclusion chromatography [15,16]. Fig. 6 shows the variation of the Kamlet–Taft π^* and β parameters for THF–CO_2 mixtures at 136 atm and 25 °C as a function of increasing proportions of CO_2. Both THF and CO_2 have negligible hydrogen-bond acidity and therefore this parameter was not measured. Similar to the methanol–CO_2 mixtures, the polarity of the mixture is similar to that of THF even when the proportion of CO_2 is as high as 60 mole fraction. Another similarity is that the π^* parameter decreases at a greater rate with increasing proportions of CO_2 than does the parameter.

Enhanced fluidity mixtures containing CO_2 are limiting in that CO_2 can react with water to form carbonic acid, may

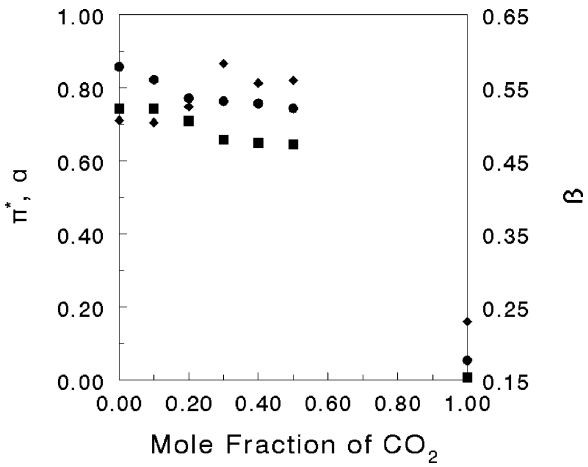

Fig. 5. Variation of Kamlet–Taft: (●) α, (◆) β, (■) π^*, with mole fraction CO_2 in the methanol–water–CO_2 mobile phase where the methanol/water ratio held at 2.3 and temperature of 25 °C and pressure of 204 atm.

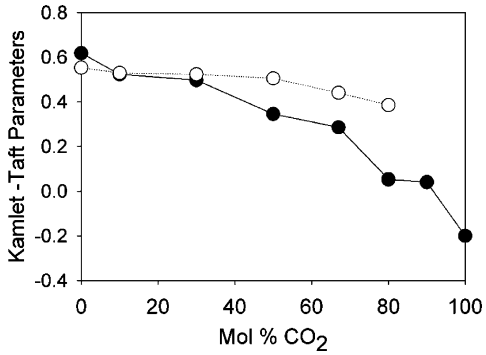

Fig. 6. Variation of the Kamlet–Taft: (●) π^* and (○) β parameter for mixtures of tetrahydrofuran–CO_2 at a pressure of 136 atm and 25 °C.

react with bases and has limited polarity. Accordingly, fluoroform has a critical condition temperature (26.2 °C) near room temperature and a low critical pressure (25.9 atm). Fluoroform is markedly more polar than CO_2 with a dipole moment of 1.651 compared to 0 for CO_2 [17]. Fig. 7A shows the variation of the Kamlet–Taft α, β, and π^* parameters for methanol and fluoroform mixtures at 170 atm and 24 °C. The general shape of the curves for the variation of hydrogen bond acidity, α, and hydrogen bond basicity, β, is similar to

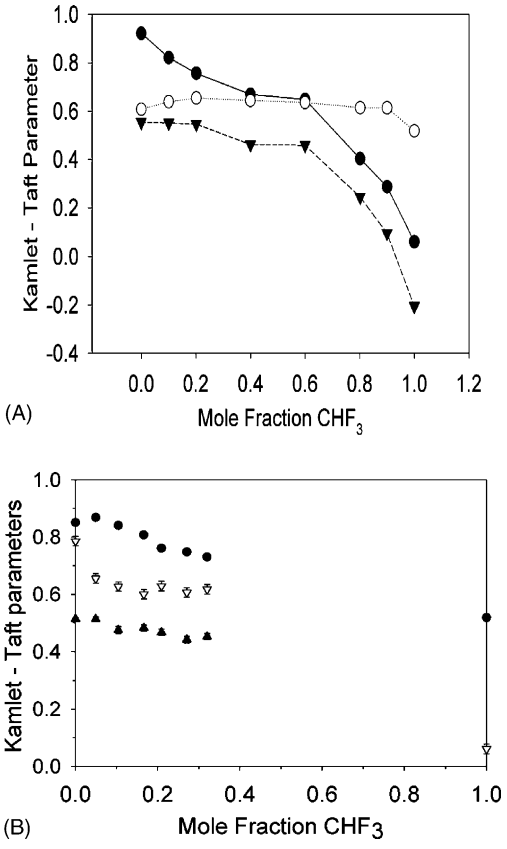

Fig. 7. A Variation of the Kamlet–Taft: (●) α, (▼) β, (○) π^* parameters for (A) methanol–CHF_3 mixtures at 170 atm and 24 °C; and (B) methanol–water–CHF_3 mixtures at (▽) α, (▲) β, (●) π^* at 170 atm and 24 °C when the methanol/water mole ratio was held constant at 1.78.

that observed for the methanol–CO_2 mixtures. However, the methanol–fluoroform mixtures have markedly lower values of and slightly lower values of for increasing proportions of the fluoroform compared CO_2. However, the π^* value varies minimally with increasing proportions of fluoroform.

Fig. 7B shows the variation of the Kamlet–Taft α, β, and π^* parameters for methanol–water–CHF_3 mixtures when the methanol–water mole ratio is held constant at 1.78 and the mole fraction of CHF_3 is varied from 0 to 32 mol%. With the water present in the mixture, the value of the π^* parameter decreases more rapidly with increasing fluoroform than that observed for the α or β parameter. However, most importantly the polarity of these mixtures remains high even when as much as 32 mol% fluoroform is in the mixture. Buffered methanol–water–CHF_3 mixtures have been used to effectively and efficiently separate highly basic analytes, such as tricyclic antidepressants, using isocratic, reversed-phase HPLC in less than half the amount of time required when using methanol–water mixtures [18].

4.2. Polarity as described by pH measurements

Using UV-Vis spectra of pH indicator molecules, such as bromophenol blue, and Eq. (3), the pH of buffered methanol–water–CO_2 enhanced-fluidity mixtures was determined [19]:

$$\frac{A_{\mathrm{HIn}}}{A_{\mathrm{In}}} \propto \frac{[\mathrm{HIn}]}{[\mathrm{In}^-]} \propto [\mathrm{H}^+] \quad (3)$$

These pH determinations were in non-aqueous solutions. Therefore, care must be taken to make certain the measured pH values are accurate. For example, in the study described above published work on pH values for methanol–water mixtures (buffered and unbuffered) were compared to those measured with our experimental setup to verify the validity of the measured pH values [20]. One other caveat to consider when using spectroscopy to measure the pH of solution is the measured absorbance values are proportional to the concentrations of analytes not proportional to the activity. If the concentrations of ions in solutions are great enough for the concentration and the activity to be significantly different, then the spectroscopy of a pH indicator is an inappropriate method of determining the pH of a solution. The ion concentrations described in the enhanced-fluidity liquid mixtures were low enough that we deemed the spectroscopic method appropriate to the analysis.

Because carbon dioxide reacts with water to form carbonic acid, the unbuffered methanol–water–CO_2 mixtures have a pH above neutral. For example, mixtures of 55.7:25.1:19.2 and 61.7:27.7:10.6 mole ratio methanol–water–CO_2 at 23 °C and 204 atm have pH values of 4.73 and 4.38, respectively. The addition of HCl to the 55.7:25.1:19.2 methanol–water–CO_2 solution to reach a concentration of 9.6×10^{-3} M HCl changed the pH to 2.96 while addition of 1.4 mM acetate buffer increased the pH to 6.41.

The importance of using buffered enhanced-fluidity mobile phases was clearly documented for substituted (2-chloro, 2-nitro, 3-hydroxyl and 4-hydroxyl) benzoic acid [21]. Using methanol–water mobile phase buffered pH = 3.00, 10.0 mM acetate buffer and a 100×2.0 mm Hypercarb, porous graphitic carbon column with 5 μm particles, the best isocratic separation was achieved in 50 min. However, with an isocratic separation using the methanol–water–CO_2 mobile phase, that included 28.8 mM phosphate buffer, baseline separation of all five substituted benzoic acids was achieved in less than 8 min. Clearly, the addition of CO_2 to the mobile phase increased the efficiency and the addition of the buffer increased the selectivity.

References

[1] S.V. Olesik, in: J.F. Parcher, T.L. Chester (Eds.), Unified Chromatography, ACS Symposium Series 748, American Chemical Society, Washington, DC, 2000, p. 168.
[2] Q. Sun, S.V. Olesik, Anal. Chem. 71 (1999) 2139.
[3] H. Yun, S.V. Olesik, Anal. Chem. 70 (1998) 3298.
[4] T.S. Reighard, S.T. Lee, S.V. Olesik, Fluid Phase Equilib. 123 (1996) 215.
[5] S.T. Lee, T.S. Reighard, S.V. Olesik, Fluid Phase Equilib. 122 (1996) 223.
[6] H. Yuan, S.V. Olesik, J. Chromatogr. A 785 (1997) 35.
[7] J. Zhao, S.V. Olesik, Fluid Phase Equilib. 154 (1999) 261.
[8] H.M. Moon, K. Ochi, K. Kojima, J. Chem. Eng. Data 40 (1995) 468.
[9] J.C. Giddings, S.L. Seager, Ind. Eng. Chem. Fundam. 1 (1962) 277.
[10] R. Feist, G.M. Schneider, Sep. Sci. Technol. 17 (1982) 261.
[11] H.H. Lauer, D. McManigill, R.D. Board, Anal. Chem. 55 (1983) 1370.
[12] I. Souvignet, S.V. Olesik, Anal. Chem. 70 (1998) 2783.
[13] S.T. Lee, S.V. Olesik, Anal. Chem. 66 (1994) 4498.
[14] M.J. Kamlet, J.L.M. Abboud, R.W. Taft, Prog. Phys. Org. Chem. 13 (1983) 485.
[15] H. Yuan, S.V. Olesik, J. Chromatogr. A 785 (1997) 35.
[16] H. Yuan, S.V. Olesik, J.Chromatogr. Sci. 35 (1997) 409.
[17] Handbook of Chemistry and Physics, 72 ed., CRC Press, Boca Raton, FL, 1991.
[18] J. Zhao, S.V. Olesik, J. Chromatogr. A 923 (2001) 107.
[19] D. Wen, S.V. Olesik, Anal. Chem. 72 (2000) 475.
[20] E. Bosch, P. Bon, H. Allemann, M. Roses, Anal. Chem. 68 (1996) 3651.
[21] D. Wen, S.V. Olesik, J. Chromatogr. A 931 (2001) 41.